Role of tetanus neurotoxin insensitive vesicle-associated membrane protein in membrane domains transport and homeostasis

Diana Molino[1,2,3,7,†,*], Sébastien Nola[1,2,3,†], Sin Man Lam[4], Agathe Verraes[1,2,3], Véronique Proux-Gillardeaux[1,2,3], Gaëlle Boncompain[5], Franck Perez[5], Markus Wenk[6], Guanghou Shui[4], Lydia Danglot[1,2,3,‡], and Thierry Galli[1,2,3,‡,*]

[1]INSERM; U950; Membrane Traffic in Health and Disease; Paris, France; [2]Univ Paris Diderot; Sorbonne Paris Cité; ERL U950; Paris, France; [3]CNRS; UMR 7592; Institut Jacques Monod; Paris, France; [4]State Key Laboratory of Molecular Developmental Biology; Institute of Genetics and Developmental Biology; Chinese Academy of Sciences; Beijing, China; [5]Institut Curie; CNRS UMR144; Paris, France; [6]Department of Biochemistry; National University of Singapore; Yong Loo Lin School of Medicine; Singapore; [7]Ecole Normale Supérieure-PSL Research University; Département de Chimie; Sorbonne Universités - UPMC Univ Paris 06; CNRS UMR 8640 PASTEUR; Paris, France.

[†]Co-first authors
[‡]Co-senior authors.

Biological membranes in eukaryotes contain a large variety of proteins and lipids often distributed in domains in plasma membrane and endomembranes. Molecular mechanisms responsible for the transport and the organization of these membrane domains along the secretory pathway still remain elusive. Here we show that vesicular SNARE TI-VAMP/VAMP7 plays a major role in membrane domains composition and transport. We found that the transport of exogenous and endogenous GPI-anchored proteins was altered in fibroblasts isolated from VAMP7-knockout mice. Furthermore, disassembly and reformation of the Golgi apparatus induced by Brefeldin A treatment and washout were impaired in VAMP7-depleted cells, suggesting that loss of VAMP7 expression alters biochemical properties and dynamics of the Golgi apparatus. In addition, lipid profiles from these knockout cells indicated a defect in glycosphingolipids homeostasis. We conclude that VAMP7 is required for effective transport of GPI–anchored proteins to cell surface and that VAMP7-dependent transport contributes to both sphingolipids and Golgi homeostasis.

Introduction

Eukaryotic cells are characterized by the occurrence of intracellular membranes which consist in lipid bilayers and monolayers confining distinct organelles. Lipids and proteins of eukaryote membranes define organelle identity, morphology and function. This organization is maintained against the constant exchanges imposed by intracellular membrane fluxes, suggesting the existence of mechanisms controlling such equilibrium based on both vesicular and non-vesicular transport. Intracellular membrane trafficking consists in 1) the fission of vesicles at a donor compartment, 2) their transport toward destination site and 3) the fusion with acceptor compartments.[1] Membrane fusion events are carried out by a family of ~40 membrane bound proteins known as SNAREs which have different subcellular localization and different regulators. SNAREs are present in vesicles (v-SNAREs) and target membranes (t-SNAREs), and the pairing of v- and t-SNAREs mediate bilayer mixing for membrane fusion. Tetanus neurotoxin-insensitive vesicle-associated membrane protein (TI-VAMP/VAMP7) is an atypical v-SNARE that in addition to the typical SNARE domain, possesses an additional N-terminal domain so-called Longin, which plays auto-inhibitory and targeting roles.[2,3] It is expressed in almost all tissues and it localizes to post-Golgi secretory vesicles, late endosomes, lysosomes and a subset of synaptic vesicles.[3] Pioneering work on VAMP7 knock down and over-expression of its regulatory

aminoterminal Longin domain have underlined its importance in several cellular processes in different cell types. VAMP7 dependent trafficking was shown to participate in apical polarity,[4] neurite growth,[5] cell adhesion,[6] transport to lysosome from both early endosomes and TGN,[7-9] cell migration, exosome and lysosomal secretion,[10,11] and autophagy.[12,13] We previously showed the involvement of VAMP7 in polarized apical transport[4,14] and its occurrence in detergent resistant membranes.[15] More recently, we showed that VAMP7 mediates transport from the Golgi apparatus to the plasma membrane (PM) particularly of tetraspanins[16] which participate in membrane organization[17] and interact with glycosphingolipids.[18] In addition, VAMP7 is involved in the transport of GLUT1 and Lat, two other membrane domain associated proteins.[19,20] Altogether, these findings led us to hypothesize a more direct contribution of VAMP7 in membrane organization and membrane domains homeostasis.

In polarized epithelial cells, GPI anchored proteins are known to be secreted apically, while the VSVG is sorted basolaterally (reviewed in [21]). Apical, but not basolateral secretion was also shown to depend upon both sphingolipids and cholesterol biosynthesis. Cholesterol and sphingolipids are known to clusters in vitro into giant vesicle and in vivo at the PM where they modulate receptor signaling and/or recycling.[22-25] Common sphingolipid precursors are ceramides, synthesized at the ER by N-acylation of sphingoid-chains with a large variety of fatty acyl-chains. This diversity is achieved by fatty acid elongation machinery, which provides fatty acids of different length, and ceramide synthase enzymes, which select fatty acid substrates based on their length. Finally ceramides are further modified by head group substitutions. In animal cells, a major pool of ceramides is used to form SM via direct addition of a phosphocholine head group. Another head group, found in all eukaryotes includes a monosaccharide such as (but not only) glucose, to form GlcCer. Further glycosylations then occur on monoglycosylated ceramides, in different Golgi subdomains,[26] to give rise to a large variety of complex glycosphingolipids (GSL) which are then transported along the secretory pathway and particularly to the PM. Sphingolipid biosynthesis and turnover are regulated with cell growth and they travel via both vesicular and non- vesicular transports from ER to Golgi, and mainly via vesicles from Golgi to PM, (for reviews see [27,28]). Secretion and sphingolipid homeostasis are co-regulated, however little is known about how a vesicular trafficking defect may impact lipids homeostasis.[27,28]

Here we found that transport of exogenous GPI-anchored proteins to the PM is inhibited and that the endogenous GPI-anchored cellular Prion protein (PrPc) accumulated in the Golgi apparatus in VAMP7 KO fibroblasts. Furthermore we found that the dynamics of the Golgi apparatus after treatment by Brefeldin A and washout was impaired in VAMP7 KO cells. KO cells also displayed modified content in sphingolipids, the biosynthesis of which is finalized in Golgi subdomains.[26] We thus propose here that VAMP7 contributes to the transport of domains' components to the cell surface, glycosphingolipids turnover and homeostatic equilibrium of Golgi.

Results

Loss of VAMP7 impairs specifically GPI transport toward PM at 37°C and more broadly Golgi-PM cargoes following low temperature block

To study the role of VAMP7 in protein secretory pathways, we ran different tests on primary mouse embryonic fibroblast (MEFs) isolated from WT and VAMP7–knockout mice. We took advantage of the RUSH assay which is based on the retention of newly synthesized proteins in the ER and their synchronized release upon addition of biotin.[29] As reporter, we used VSVG– and GPI–anchored mCherry-tagged fluorescent proteins, which are expected to segregate at the exit of the Golgi and follow different routes from the Golgi toward the PM.[30] One hour after biotin addition at 37°C, surface staining intensity of mCherry-VSVG in WT and KO cells was similar while mCherry-GPI surface signal was strongly reduced in KO compared to WT, suggesting that GPI-anchored proteins transport toward the PM was delayed in KO (Fig. 1 A-D).

To further investigate defects in Golgi-to-PM secretory pathway, we used low temperature block to synchronize membrane fluxes by preventing cargo exit from donor compartment. Using a 20°C block protocol, we previously observed an accumulation of VAMP7 at the Golgi in Cos7 cells [31] and a delayed transport of tsO45VSVG (a thermosensitive mutant form of VSVG [32]) to the cell surface in VAMP7 knocked-down HeLa cells.[16] We thus coupled the RUSH assay with the 20°C temperature block experiment (**Fig. 2**). In such conditions, the PM release of both GPI and VSVG was significantly inhibited in KO compared to WT (**Fig. 2B–E**). Altogether, these data indicate that VAMP7 KO MEFs are not able to properly sort GPI-anchored proteins from the Golgi to the cell surface at physiological temperature and both VSVG and GPI after 20°C temperature block.

To check whether or not this effect could be due to a transport defect or latency in the early secretory pathways (i.e from ER to ERGIC, and from ERGIC to the Golgi apparatus), we used the RUSH assay with short biotin incubation time (less than 30min) and monitored the arrival of VSVG and GPI in the Golgi apparatus by counterstaining with GM130 antibody (**Fig. 3A**). As previously reported,[33] 20 minutes after biotin addition, both VSVG and GPI accumulated in the Golgi in WT as well as KO cells. We quantified the amount of GPI or VSVG present in GM130-positive area and observed no significant difference between WT and KO for every tested conditions (unstimulated, 10, 20 and 30 min of biotin addition) (**Fig. 3B**) indicating that the GPI retention previously observed in the KO does not come from a defect in the ER and likely relates to post-Golgi transport to the cell surface. These data suggest that GPI-anchored proteins and VAMP7 should be transported together from the Golgi area to the periphery. In order to directly test this hypothesis, we expressed GPI–anchored mCherry of the RUSH assay and GFP-VAMP7 in HeLa cells which are better prone to multiple transfection than MEFs. Following the addition of biotin, mCherry-GPI was released from the ER and accumulated in the Golgi after 40 min. Time-lapse imaging showed initial extensive colocalization in a perinuclear area likely corresponding to the

Golgi apparatus followed by some co-labeled vesicles which, with time, were more found at the cell periphery (**Movie S1**).

To confirm the role of VAMP7 on GPI-anchored protein transport, we monitored the steady state endogenous localization of the prion protein PrPc, a well-known GPI-anchored protein involved in the development of prion encephalopathy.[34] Immunostaining revealed that endogenous PrPc signal in the Golgi region (marked by Golgin A4) was increased in KO MEFs compared to WT (**Fig. 4A–C**), suggesting that lack of VAMP7 causes partial retention of PrPc in the Golgi apparatus. In order to establish the specificity of the effect of deleting VAMP7 on GPI-anchored proteins post-Golgi transport, we expressed exogenous GFP-tagged VAMP7 in WT and KO MEFs. This led to a clear disappearance of PrPc accumulation in the Golgi area and a diffuse staining indicating normal transport to the cell surface (**Fig. 4B,C**). VAMP7 thus appears to be required for the correct transport of GPI-anchored proteins from the Golgi apparatus to the plasma membrane.

Loss of VAMP7 affects Golgi dynamics

Interestingly, although not fully clarified, low temperature is believed to prevent sorting at Golgi, likely because of impaired membrane budding.[35] Thus, the higher sensitivity of VAMP7 KO cells for the 20°C block suggests that VAMP7 may play a role in Golgi biochemical properties and homeostasis. Furthermore, a recent study from a medium scale RNAi screen identified human sybl1 (encoding for VAMP7) as one of the hits leading to cis Golgi compactness defect.[36] Therefore, we sought to assay for a structural and/or dynamic defect of the Golgi in the absence of VAMP7 expression. To this aim, WT and VAMP7 KO MEFs transiently expressing GFP-tagged N-acetyl-glucosaminyl-transferase (NAGT-GFP) were treated with BFA, a drug known to reversibly disrupt the Golgi apparatus and causes resident enzymes such as NAGT-GFP, to diffuse back to the ER [37] (**Fig. 5A**). Cells were monitored by live imaging and we computed the variation of the number of objects positive for NAGT-GFP during BFA treatment and washout as a way to quantify Golgi disassembly and reformation. In WT cells, the number of NAGT-GFP positive objects dropped during the BFA treatment and was restored following washout in agreement with Golgi disassembly-
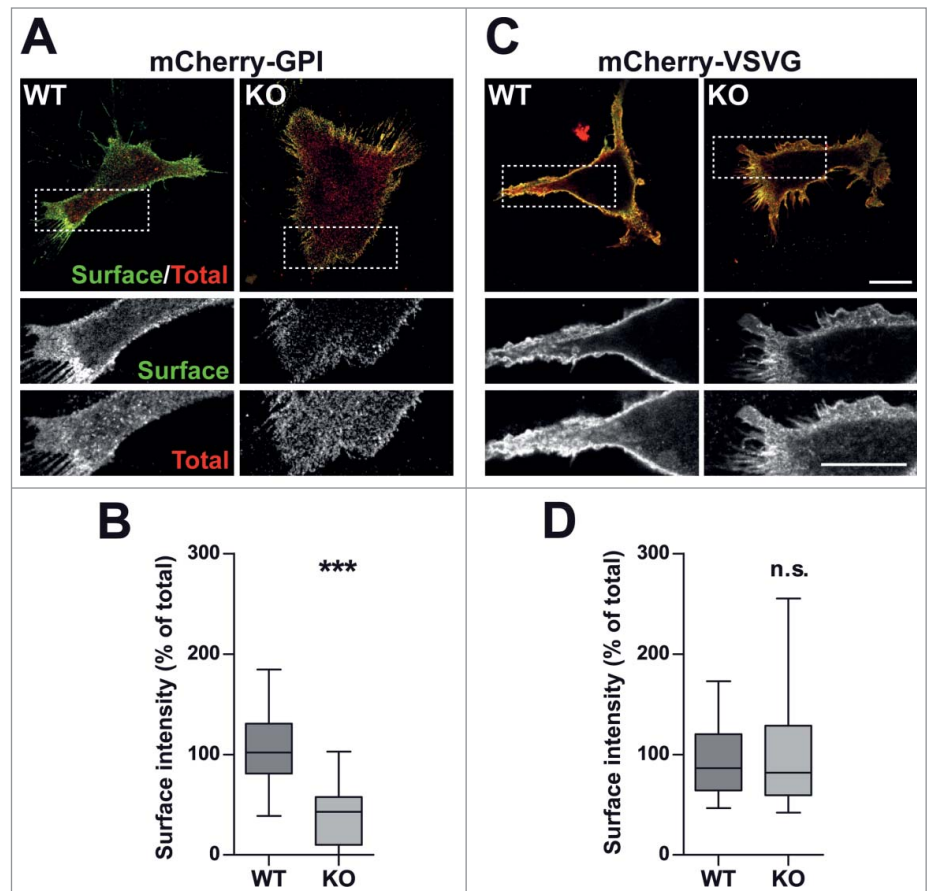

Figure 1. Loss of VAMP7 impairs the secretion of GPI anchored protein at physiological temperature-MEFs from WT and KO were transfected with either mCherry-GPI or mCherry-VSVG constructs of the RUSH system. Biotin release was induced at 37°C for 1 h. (**A** and **C**), Surface immunostaining (green) of mCherry-GPI (**A**) or mCherry-VSVG (**C**) was performed and the total pool of proteins (red) was revealed by immunodetection. Lower panels display the magnification indicated by dotted outlines in corresponding top panels. (**B** and **D**), Box plots (25th/75th percentiles, medians as horizontal lines, 5th/95th percentiles values as vertical bars) showing quantifications of **A** and **C**, respectively. The rate of exocytosis of mCherry-GPI (**B**) or mCherry-VSVG (**D**), was measured by calculating the ratio between surface and total pool integrated signals, which are represented in graphs as % of WT. Data shown are from 3 independent experiments, using a total of 3WT and 3KO culture with 10–12 cells for each embryo. Bar, 20 μm. Significance was determined by Mann Whitney test. ***, $P < 0.001$; n.s., not significant.

reformation paradigm. In contrast, NAGT-GFP particle number remained significantly higher during BFA treatment as well as in early timepoints of washout in KO cells. Both WT and KO recovered to the same endpoint. The delayed recovery in KO cells suggests that the VAMP7 KO impacts BFA-dependent mechanisms in the Golgi apparatus. Altogether, these results suggest that the loss of VAMP7 has profound effects on dynamic properties of the Golgi.

Loss of VAMP7 affects cell sphingolipidome

Golgi membranes represent a reservoir of lipids and proteins and contain many keys enzymes for the processing of both lipids and proteins. Glycosphingolipid biosynthesis is completed at the Golgi apparatus [26] and GPI biosynthesis was suggested to be needed for sphingolipid biosynthesis at the ER in yeast.[38] We
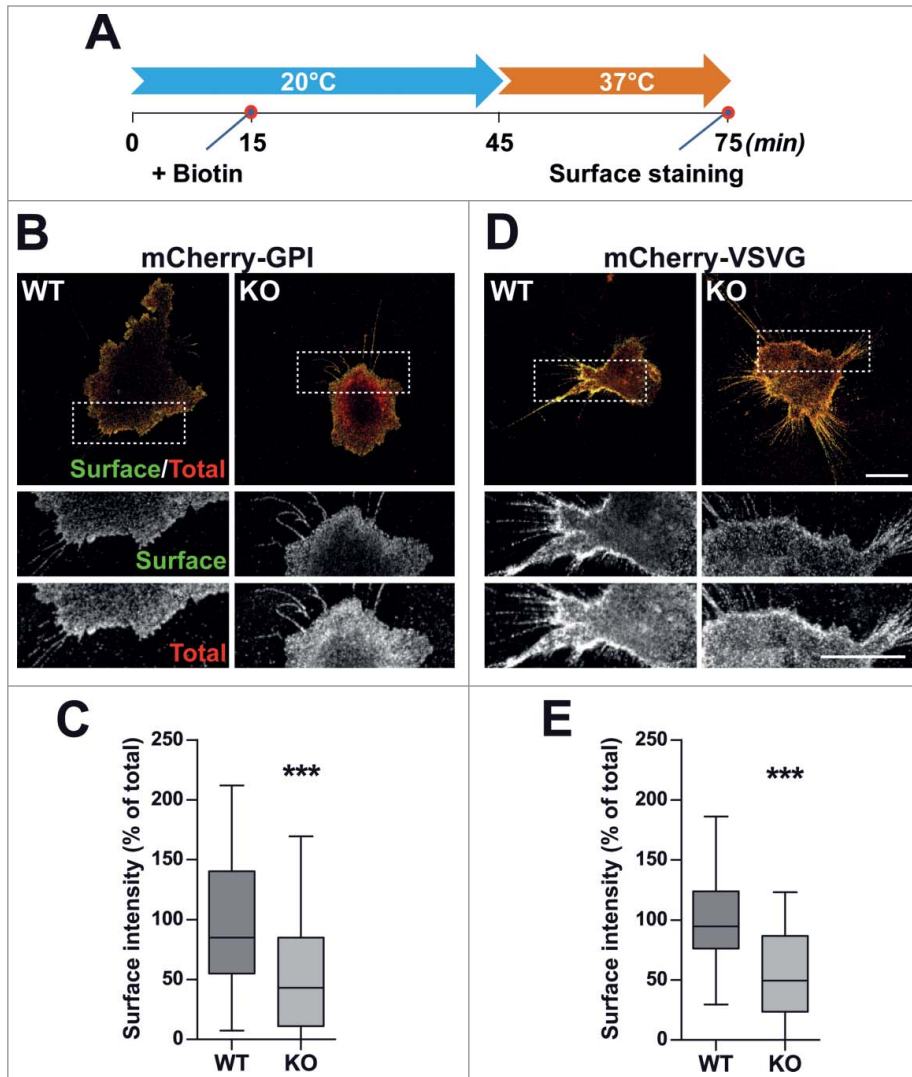
Figure 2. Loss of VAMP7 impairs the secretion of GPI-anchored protein and VSVG after 20°C block-MEFs from WT and KO were transfected with either GPI-Cherry or VSVG-Cherry plasmids of the RUSH system. Biotin release was induced after cell acclimation at 20°C and after 30 min, cells were then shifted to 37°C for further 30 min (**A**). The last timepoint (1 h) was used for quantifications. (**B** and **D**), Surface immunostaining (green) of mCherry-GPI (**B**) or mCherry-VSVG (**D**) was performed and the total pool of proteins (red) was revealed by further immune detection. Lower panels display the magnification indicated by dotted outlines in corresponding top panels. (**C** and **E**), Box plots showing quantifications of **B** and **D**, respectively. The rate of exocytosis of mCherry-GPI (**B**) or mCherry-VSVG (**D**), was measured by calculating the ratio between surface and total pool integrated signals, which are represented in graphs as % of WT. Data shown are from 3 independent experiments, using a total of 3WT and 3KO culture with 10–12 cells for each embryo. Bar, 20 μm. Significance was determined by paired t-test. ***, $P < 0.001$.

(**Table S1**). Differently, long chain-SM were unaffected in KO and very long SM where instead reduced (**Table 1** and **Table S1**), suggesting a preferential channeling of very long chain ceramides (VLC-Cer) precursors to form VLC-GM3, with concomitant reduction of VLC-SM in VAMP7-KO MEFs. Altogether these results suggest a crosstalk between VAMP7-dependent vesicular transport and glycosphingolipid homeostasis.

Discussion

The results shown here unravel a role of TI-VAMP/VAMP7 in Golgi apparatus homeostasis and post-Golgi trafficking. We found that exogenous and endogenous GPI-anchored proteins transport to the plasma membrane was delayed in VAMP7 knockout MEF and that Golgi accumulation of PrPc in the Golgi was rescued by restoration of VAMP7 expression in KO cells. This delay appeared to result from defect in transport and/or modification in the Golgi apparatus, and was not found to be related to ER-Golgi export defect. Time-lapse videomicroscopy showed the occurrence of GPI- and VAMP7 positive post-Golgi vesicles. Furthermore we found that the Golgi dynamics were impaired and sphingolipid homeostasis perturbed in VAMP7 KO cells. Our phenotypic analysis of VAMP7 KO MEFs thus suggests an original functional correlation between the transport of membrane domain proteins (GPI-anchored proteins), GSL homeostasis and Golgi apparatus dynamics. These three cellular phenotypic traits may be connected solely functionally or more directly via protein-protein and protein-lipid interactions and regulations.

The search of its molecular network showed that VAMP7 interacts with Varp (a Rab21 guanine nucleotide exchange factor), which itself binds to the molecular motor Kif 5, both being involved in directing movement of VAMP7 vesicles from the cell center to the cell periphery.[31,39] Our time-lapse imaging experiment clearly indicates that GPI-anchored proteins are to a certain extent in VAMP7-positive vesicles following their exit from the TGN, suggesting co-transport outbound the Golgi. In addition, Varp interacts with Vps29, a subunit of the retromer, and both are involved in the

thus asked to which extent VAMP7 KO-dependent Golgi apparatus-related above mentioned defects may also impact sphingolipid homeostasis. For an overall understanding we analyzed lipid profiles of WT and KO MEFs cells by HPLC-MRM and found major changes in sphingolipid profiles (**Table 1**). Different GM3 species including GM3 containing long (C16-18) or very long acyl chain (C ≥ 20) were both increased in KO. Ceramides, precursors of both GM3 and SM, were also increased in the KO (**Table 1**), while phospholipid profiles were rather unchanged

transport of the glucose transporter GLUT1 to the PM whereas VAMP7 is involved in exocytosis of both GLUT1 and GLUT4.[19,40] GLUT1 and GLUT4 are known to function in membrane domains.[41,42] In addition, phospholipase D1 (PLD1) is transported in VAMP7 vesicles, controls its fusion capacity [43] and is an effector of Arf1 [44,45] so that the absence of VAMP7 could alter Golgi lipidic content and confer BFA-resistance via an accumulation or altered activity of PLD1 at the TGN. The activity of other enzymes involved in lipid metabolism particularly those regulating GSL biosynthesis at the Golgi might be also altered as a result of the absence of VAMP7 (see below). VAMP7 was further recently identified on vesicles transporting newly synthesized lysosome-associated membrane proteins directly from the TGN to late endosomes.[9] These vesicles contained both late endosome markers and VAMP7 indicating an alternative pathway from trans-Golgi network to late endosomes. Thus a role of VAMP7 in transport of membrane domain component at the exit of the Golgi apparatus, as suggested here, is in good agreement

Figure 3. Loss of VAMP7 does not affect ER-to-Golgi transport of GPI-anchored and VSVG proteins (**A** and **C**), MEFs from WT and KO were transfected with either mCherry-GPI (**A**) or mCherry-VSVG (**C**) plasmids of the RUSH system. ER release was induced with biotin addition at 37° for 10, 20 or 30 minutes. MEFs from WT and KO were fixed and immunostained with Golgi marker anti-GM130 and -GFP or -mCherry antibodies to record proteins reaching and passing the Golgi. Top left inserts show magnification of the Golgi region. (**B** and **D**), for each timepoint, integrated signal intensity mCherry or GFP at Golgi was deducted from a GM130 mask and divided by total cell corresponding integrated signal. Data shown are mean ± SEM of samples from 2 independent experiments with 2WT and 2 KO culture, with at least 10 cells for each embryo and per timepoint. Significance was determined by 2-way ANOVA with Bonferroni's post-test; n.s., not significant.

with roles in both exocytosis toward PM and transport to late endosomes and opens new perspective on the possible sorting pathways followed by sphingolipids.

The present demonstration of the role of VAMP7 in GPI-anchored proteins transport to the cell surface strengthens the finding that VAMP7 depletion leads to decreased expression of the tetraspanin CD82 at the cell surface, which in turn impacts EGFR function at the PM.[16] Tetraspanins are also known to form a specific kind of membrane domains,[46] interact with GSL [18,47] and modulate EGFR signaling.[48] Therefore, TI-VAMP-

dependent regulation of EGFR may result from its role in transport of components of membrane domains.

In a previous work we had found that knockdown of VAMP7 expression impaired VSVG-tsO45 secretion using the classical temperature shift assay from 39°C to 20°C.[16] Here, we took advantage of the RUSH assay,[33] and we identified a secretion defect of GPI-anchored proteins but not VSVG at physiological temperature (37°C). However at 20°C, using the RUSH system, the secretion of both proteins was impaired in KO vs WT. Temperature as low as 20°C have been widely used in cell
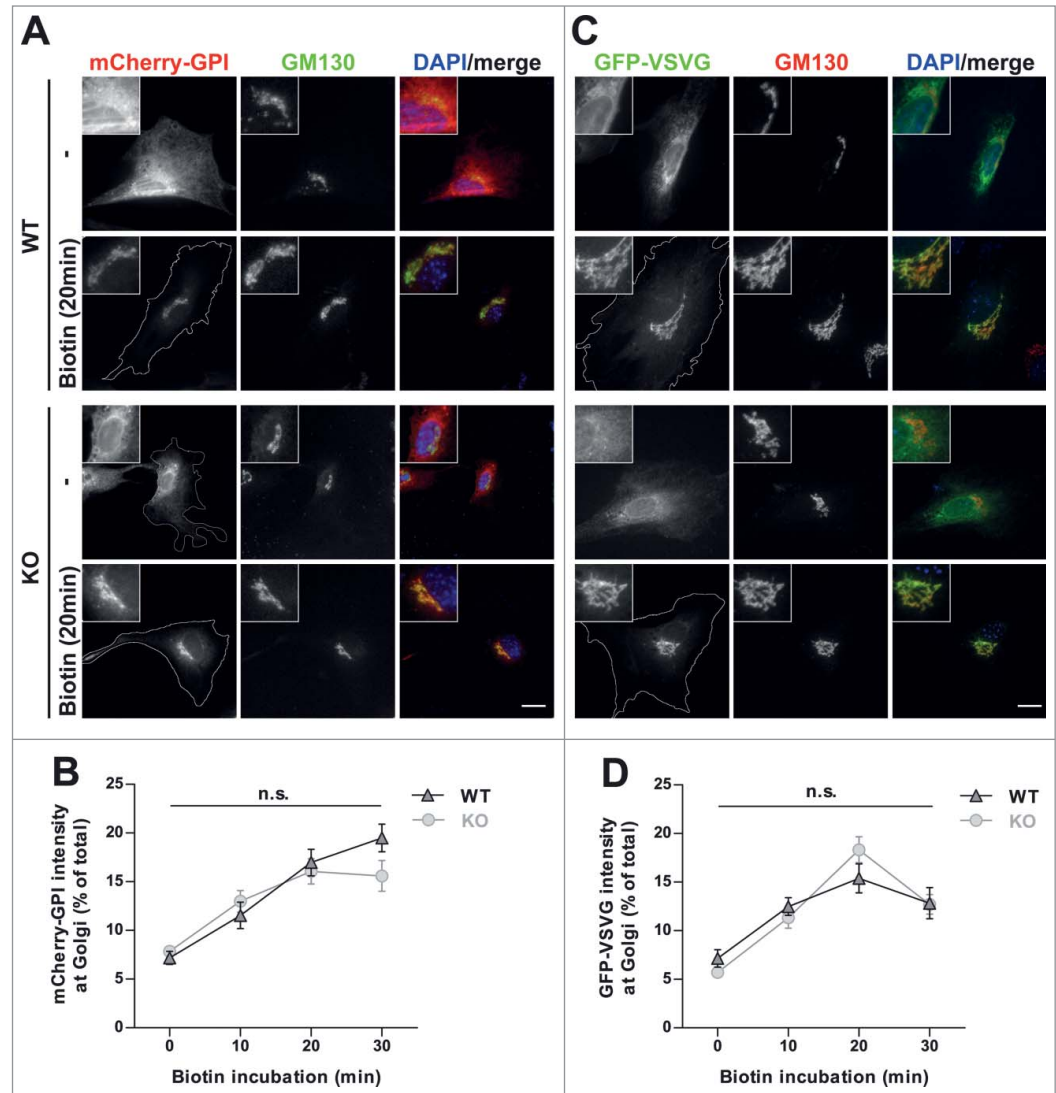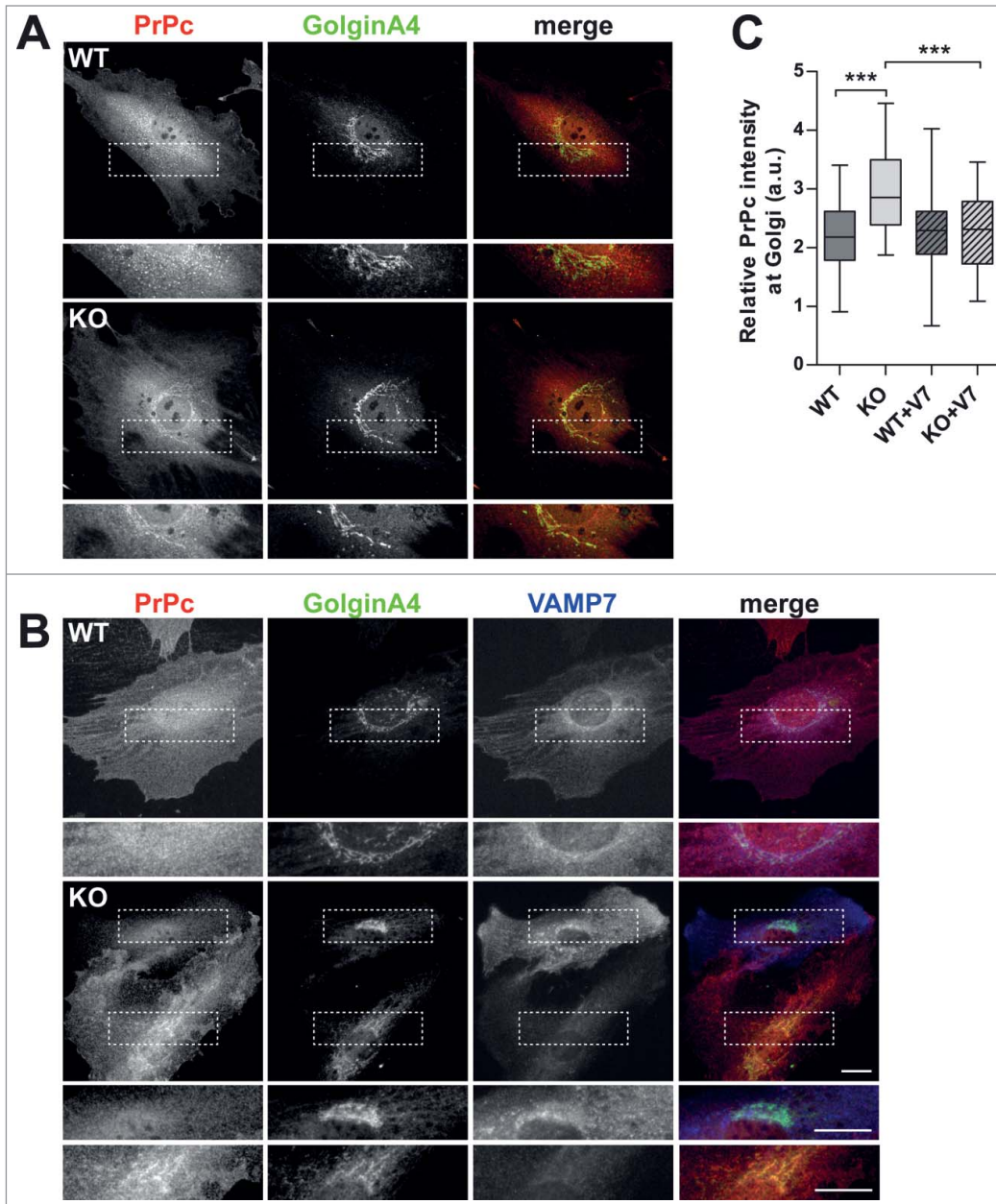
Figure 4. Accumulation of PrPc in the Golgi apparatus in VAMP7 KO MEFs (**A** and **B**) MEFs KO for VAMP7 and WT, overexpressing (**B**) or not (**A**) GFP-VAMP7 were fixed and immunostained with anti-PrPc and anti-GolginA4 antibodies. GFP-VAMP7 is false-colored in blue to simplify visualization. Dotted-line boxes represent magnification region displayed at the bottom of each panel. (**C**) For each cell, ratio between mean intensity of PrPc signal in Golgi region (obtained via a Golgin A4 mask) and total cell PrPc signal (cell mask) was calculated and represented as box plots. Data shown are from 3 independent experiments, using a total of 3WT and 3KO culture with 25 cells per embryo. Bar, 20 µm. Significance was determined by one-way ANOVA test with Bonferroni's post-test. ***: $P < 0.001$.

anchored proteins are segregated at the Golgi with and without a temperature block [30] and that a kinase dead mutant PKD an α-SNAP mutant and tannic acid treatment induced the colocalization of VSVG and GPI-anchored proteins in the same post-Golgi carriers.[53] It is possible that such temperature-dependent mis-sorting occurs in VAMP7 KO as a result from GSL defect in the Golgi apparatus. Indeed, GlcCer is produced in the cytosolic leaflet of early Golgi membranes and is transported across the Golgi either via a vesicular pathway or directly with the FAPP2 lipid transfer protein.[54] It has been proposed that these 2 differently transported GlcCer pools follow 2 different glycosylation mechanisms in different Golgi regions. In particular, GlcCer transported by direct protein transfer is used to synthesize glycosphingolipids known as globosides in the TGN while vesicular transported GlcCer is used in the Golgi cisternae for ganglioside production such as that of GM3.[26] Along this line, an attractive hypothesis could be that complex GSL biosynthesis and GPI-anchored proteins may share similar intra- and/or outward-Golgi vesicular pathways, which would be VAMP7-dependent, and may be directly involved in Golgi homeostasis and dynamics.

In conclusion, VAMP7 KO MEFs show phenotypes clearly related to the traffic of lipids and proteins known to reside in membrane domains. While these phenotypic traits do not preclude cell and organism life,[55,56] they may nevertheless induce profound signaling defects [20] which largely remain to explore. Further studies are required to address the impact of this mechanism in the organism and also how a v-SNARE which primarily mediates membrane fusion may also be required at earlier stages

biology.[49,50] Below 20°C membrane viscosity is changed, endocytosis is impaired, degradation is delayed due to defective transport to the lysosome[51] and secretion is also delayed likely because of budding defect at the Golgi generating increased cargo load.[35,52] Thus, we envision this temperature-dependent difference as a consequence of both modified GSL contents and accumulated protein cargoes (i.e. GPI-anchored proteins) in VAMP7 KD and KO cells. It is intriguing that VSVG and GPI-
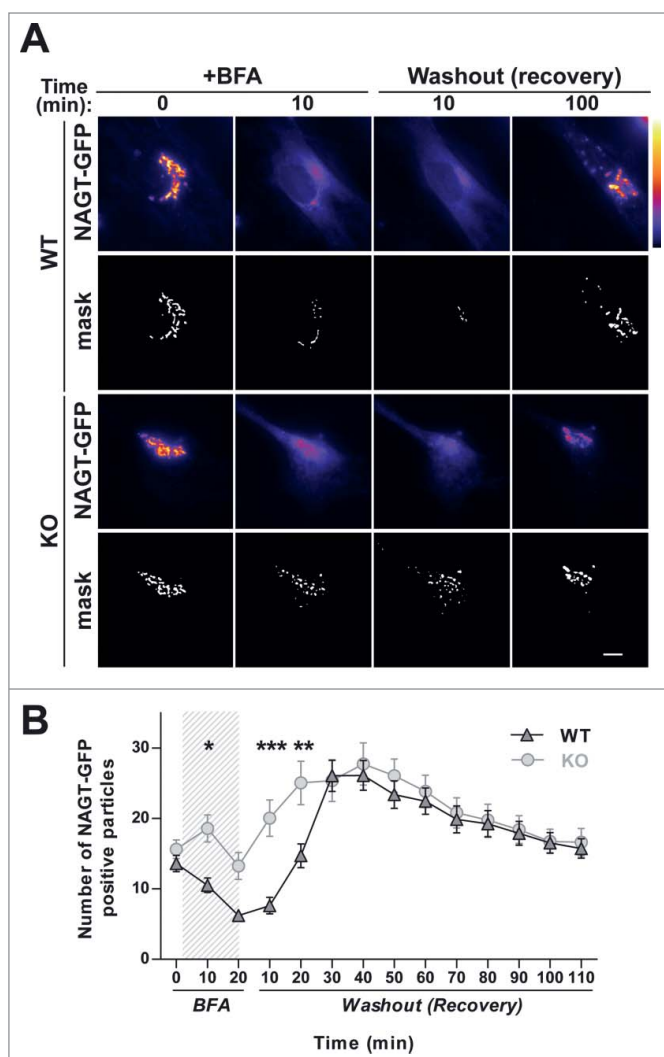
Figure 5. Loss of VAMP7 impairs BFA-evoked disassembly/reassembly of the Golgi apparatus. MEFs from WT and VAMP7 KO expressing NAGT-GFP construct were monitored by live cell imaging following BFA treatment and washout. (**A**) Representative snapshots are displayed as false-colored images for better contrast (top panels). Corresponding binary mask obtained by wavelet-based segmentation (see Experimental procedures) are shown in lower panels. (**B**), Number of NAGT-GFP positive particles was measured and used as an indicative parameter for BFA sensitivity and Golgi dynamics (i.e., recovery of compartment morphology after washout). Data are from 3 independent experiments, using a total of 3 WT and 3KO cell culture with approximately 10 cells per embryo. Bars, 10 μm. Significance was determined by 2-way ANOVA with Bonferroni's post-test. *: $P < 0.05$, **: $P < 0.01$, ***: $P < 0.001$.

of membrane traffic like sorting of some components of membrane domains.

Materials and Methods

Primary cell isolation, culture and transfection

Primary embryonic fibroblasts (MEFs) were harvested from WT and VAMP7 KO littermate E15 male embryos from crossing between KO males with females VAMP7 -/+ which were previously backcrossed (>11) on C57BL/6 background.[56] All animals were handled in strict accordance with good animal practice as defined by the national and/or local animal welfare bodies including local Ethics Committee (called CEEA40-*Comité d'éthique Buffon* at the Ministry of Higher Education and Research), and all mouse work was approved by the Veterinary Services of Paris (Authorization number: 75-1073). Because VAMP7 gene is located on the X chromosome, only male embryos were used for cell culture. Cells were cultured in Dulbecco's modified Eagle's medium with 4.5g/L glucose and pyruvate (GIBCO, Invitrogen), supplemented with 10% fetal bovine serum, 2mM L-Glutamine, 10 units/penicillin and 10 μg/ml streptomycin, in a 5% CO_2-humidified atmosphere at 37°C and split at least 3 times to enrich the fibroblast population. Experiments were performed before passage 6. Cells were transfected with either JetPrime (Polyplus transfection) or Lipofectamine 2000 (Invitrogen) according to manufacturer's instructions.

Immunofluorescence studies and antibodies

For classical immunolocalization studies cells were fixed with PFA 4% at room temperature then washed 5 times in PBS and incubated with NH4Cl 50 mM in PBS for 20 min. Cell were then permeabilized with 0,1% Triton-PBS, extensively washed and blocked for 30 min with Fish Gelatin 0,25% in PBS. Primary antibodies were incubated overnight at 4°C in PBS-gelatin 0,125%. Primary Ab used included mouse anti-GM130 (Transduction Lab), anti-STX6 (Transduction Lab), anti-PrPc (SAF32, kind gift of Jacques Grassi, CEA, Fontenay-aux-Roses, France), anti-mCherry (Clontech), rabbit anti-GolginA4 (kind gift of Mickey Marks, University of Pennsylvania School of Medicine, Philadelphia, USA [57]) and goat anti-mCherry (Acris). Secondary antibodies coupled to Alexa488 (Invitrogen), CY3 or CY5 (Jackson Laboratories) were incubated for 1 h at room temperature.

Confocal microscopy

Fixed cells were imaged with LSM 710 (Zeiss) confocal microscope, using a 405 nm diode laser line exciting DAPI, a 488 nm argon laser line exciting Alexa Fluor 488 and a 561 nm diode laser line exciting CY3. Emission was detected between 410 and 480 nm for DAPI, 495–530 nm for Alexa Fluor 488 and 565–600 nm for CY3.

BFA treatment and live cell imaging

WT and KO MEFs were cultured on 30 mm diameter coverglass and transfected with NAGT-GFP construct. Live cell imaging was conducted 16 to 24 h post-transfection in modified Krebs-Ringer-HEPES buffer (135 mM NaCl, 2.5 mM KCl, 1.2 mM MgCl2, 1 mM CaCl2, 20 mM HEPES, 11.1 mM glucose, pH 7.4) supplemented with 1% FBS. Cells were imaged at 37°C using an inverted Leica DMI6000B microscope (Leica Microsystems, Manheimm, Germany), equipped with a 63X/1.4-0.6 NA Plan-Apochromat oil immersion Leica objective, an EMCCD digital camera (Cascade:512B; Roper Scientific,

Table 1 Sphingolipidome of WT and KO cell cultures indicates role of VAMP7 in sphingolipid homeostasis

	Lipids	WT		KO		P value	Significativity	KO/WT
		AVERAGE	ST.DEV	AVERAGE	ST.DEV			
LC-SM	SM18:1/16:1	3.8567	0.0773	4.2774	0.2666	P > 0,05	ns	
	SM18:1/16:0	34.9759	5.6531	37.5035	4.6819	P > 0,05	ns	
	SM18:0/16:0	7.3345	0.3818	8.2567	0.7237	P > 0,05	ns	
	SM18:1/18:1	0.5983	0.0305	0.7062	0.0808	P > 0,05	ns	
	SM18:1/18:0	4.2823	0.3814	4.0392	0.1480	P > 0,05	ns	
	SM18:0/18:0	22.6728	3.1238	22.2069	2.4441	P > 0,05	ns	
VLC-SM	SM18:1/20:1	1.0376	0.0986	0.9941	0.0025	P > 0,05	ns	
	SM18:1/20:0	**7.5537**	**1.0747**	**6.2917**	**0.6126**	**P < 0,01**	******	↓
	SM18:1/22:1	2.1680	0.2758	1.8193	0.3453	P > 0,05	ns	
	SM18:1/22:0	**8.1332**	**0.5501**	**5.5142**	**0.0901**	**P < 0,001**	*******	↓
	SM18:1/24:1	**2.4540**	**0.3936**	**1.4243**	**0.3118**	**P < 0,05**	*****	↓
	SM18:1/24:0	1.3681	0.1403	0.7575	0.1292	P > 0,05	ns	
	SM18:0/24:0	0.2657	0.0237	0.1648	0.0204	P > 0,05	ns	
LC-Cer	**Cer d18:1/16:0**	**2.8158**	**0.4450**	**4.1864**	**0.1801**	**P < 0,001**	*******	↑
	Cer d18:0/16:0	0.1069	0.0252	0.1382	0.0074	P > 0,05	ns	
	Cer d18:1/18:0	0.1681	0.0248	0.2370	0.0466	P > 0,05	ns	
	Cer d18:0/18:0	0.0042	0.0010	0.0052	0.0008	P > 0,05	ns	
VLC-Cer	Cer d18:1/20:0	0.0257	0.0111	0.0336	0.0050	P > 0,05	ns	
	Cer d18:0/20:0	0.0010	0.0005	0.0010	0.0001	P > 0,05	ns	
	Cer d18:1/22:0	0.0307	0.0083	0.0545	0.0179	P > 0,05	ns	
	Cer d18:0/22:0	0.0011	0.0002	0.0015	0.0001	P > 0,05	ns	
	Cer d18:1/24:1	**0.0433**	**0.0035**	**0.0769**	**0.0036**	**P < 0,01**	******	↑
	Cer d18:1/24:0	0.0507	0.0204	0.0649	0.0286	P > 0,05	ns	
	Cer d18:0/24:1	0.0015	0.0006	0.0017	0.0003	P > 0,05	ns	
	Cer d18:0/24:0	0.0018	0.0004	0.0020	0.0002	P > 0,05	ns	
LC-GM3	**GM318:1/16:0**	**4.3834**	**0.4000**	**6.4004**	**0.7342**	**P < 0,001**	*******	↑
	GM318:0/16:0	0.7336	0.1314	1.0182	0.1778	P > 0,05	ns	
	GM318:1/18:1	0.0467	0.0097	0.0532	0.0130	P > 0,05	ns	
	GM318:1/18:0	0.2717	0.1044	0.3281	0.1338	P > 0,05	ns	
	GM318:0/18:0	0.0489	0.0201	0.0796	0.0324	P > 0,05	ns	
VLC-GM3	GM318:1/20:1	0.0154	0.0020	0.0233	0.0129	P > 0,05	ns	
	GM318:1/20:0	0.0853	0.0262	0.1237	0.0537	P > 0,05	ns	
	GM318:0/20:0	0.0233	0.0061	0.0671	0.0078	P > 0,05	ns	
	GM318:1/22:1	0.0677	0.0110	0.1076	0.0268	P > 0,05	ns	
	GM318:1/22:0	**0.2371**	**0.0792**	**0.4983**	**0.0810**	**P < 0,05**	*****	↑
	GM318:0/22:0	0.0565	0.0174	0.1316	0.0426	P > 0,05	ns	
	GM318:1/24:1	**0.6108**	**0.2539**	**1.3212**	**0.1776**	**P < 0,001**	*******	↑
	GM318:1/24:0	**0.5450**	**0.2454**	**1.1670**	**0.1126**	**P < 0,001**	*******	↑
	GM318:0/24:0	0.0859	0.0288	0.2181	0.0439	P > 0,05	ns	
PI	PI 34:2	1.331	0.273	1.128	0.263	P > 0,05	ns	
	PI 34:1	1.774	0.233	1.343	0.111	P > 0,05	ns	
	PI 36:4	0.589	0.173	0.667	0.125	P > 0,05	ns	
	PI 36:3	1.696	0.417	1.748	0.469	P > 0,05	ns	
	PI 36:2	5.486	1.441	5.572	0.861	P > 0,05	ns	
	PI 36:1	2.428	0.453	2.351	0.087	P > 0,05	ns	
	PI 38:5	2.361	0.374	2.394	0.103	P > 0,05	ns	
	PI 38:4	5.437	0.676	5.886	0.267	P > 0,05	ns	
	PI 38:3	4.437	0.940	4.475	0.917	P > 0,05	ns	
	PI 40:6	0.399	0.051	0.350	0.015	P > 0,05	ns	
	PI 40:5	0.479	0.069	0.453	0.019	P > 0,05	ns	
	PI 40:4	0.354	0.037	0.300	0.018	P > 0,05	ns	

Trenton, NJ) and controlled by Metamorph software (Roper Scientific).

For BFA experiments, cells were treated with 5 μM BFA for 20 min, and then extensively washed by imaging buffer perfusion for 10 min. Acquisition started with BFA addition and was performed every 10 min for 2 h. For quantification, NAGT-GFP signal was segmented using "Wavelet spot detector" module of Icy imaging software (http://www.bioimageanalysis.org/) [58] and particle analysis of resulting masks was processed in ImageJ (imagej.nih.gov/ij/).

For dynamic study of mCherry-GPI RUSH and GFP-VAMP7 co-expressed in Hela cells, acquisition started 40 min after biotin addition and images were taken every 5 min for 150 min. Binary masks of each channel were obtained using Icy "Wavelet spot detector" analysis. Channels merging and movie montage were performed with ImageJ.

Secretion assays

For secretion studies, cells were transfected with mCherry-tagged GPI and VSVG constructs of the RUSH system generated by Boncompain et al.[29] 24 h after transfection, secretion was induced with 40 μM Biotin (Sigma Aldrich). After induced release cells were quickly washed at 4°C with DMEM buffered with 20 mM HEPES and then incubated in the same solution with primary mouse anti-mCherry antibody for 20 min at 4°C to allow surface epitope labeling. Cells were then washed, fixed with PFA 4%, and incubated with secondary Alexa488 antibody. To reveal the total pool, cells were than permeabilized with 0,1% Triton X-100 and re-incubated with the same primary anti-mCherry antibody and a CY3-coupled secondary antibody following the classical immunofluorescence procedure. This protocol allows distinguishing the fraction of protein secreted at the surface (Alexa Fluor 488 staining) and the total amount of expressed protein (CY3 staining) for evaluating the efficiency of secretion. To this aim, after thresholding, integrated intensity of each channel was measured with ImageJ and a ratio between Cy3 and Alexa Fluor 488 integrated signals was calculated.

Analysis of lipids using high performance liquid chromatography/mass spectrometry

Lipid analysis was carried as previous described.[59] Briefly, 750 μl of ice cold chloroform: methanol (1:2, v/v) was added to cells resuspended in 100 ul of PBS. The mixture was vortexed vigorously for 1 min. After mixing at 1200 rpm at 4 oC for 1 hour, 250 μl ice cold chloroform and 350 μl of ice cold water was added to the samples. The samples were then subjected to another 1 min vortexing. After centrifugation at 9000 rpm for 2 min, the lower organic phase was collected. Lipids were re-extracted from the remaining aqueous phase with 450 μl of ice cold chloroform. The two extracts were pooled and vacuum-dried. An Agilent high performance liquid chromatography (HPLC) 1260 system coupled with an Applied Biosystem Triple Quadrupole/Ion Trap mass spectrometer (4500 Qtrap) was used for quantification of individual lipid. Individual lipid species were quantified by referencing to spiked internal standards. PC-14:0/14:0, PE-14:0/14:0, PS-34:1/d31, PG-14:0/14:0, PI-34:1/d31, C17 ceramide, C8 glucosylceramide and SM 18:1/12:0 were obtained from Avanti Polar Lipids (Alabaster, AL, USA).

Data processing and statistics

Data were processed first with Wilcoxon test to evaluate data distributions. Data with Gaussian distributions were validated with paired t-test, non-Gaussian distributed sets of data were evaluated with Mann Whitney or ANOVA tests as specified in figure legends. Graphs and statistics were obtained using GraphPad Prism software.

Supplemental Material

Supplemental data for this article can be accessed on the publisher's website.

References

1. Bonifacino JS, Glick BS. The mechanisms of vesicle budding and fusion. Cell 2004; 116:153-66; PMID:14744428; http://dx.doi.org/10.1016/S0092-8674(03)01079-1
2. Martinez-Arca S, Alberts P, Zahraoui A, Louvard D, Galli T. Role of tetanus neurotoxin insensitive vesicle-associated membrane protein (TI-VAMP) in vesicular transport mediating neurite outgrowth. J Cell Biol 2000; 149:889-900; PMID:10811829; http://dx.doi.org/10.1083/jcb.149.4.889
3. Chaineau M, Danglot L, Galli T. Multiple roles of the vesicular-SNARE TI-VAMP in post-Golgi and endosomal trafficking. FEBS Lett 2009; 583:3817-26; PMID:19837067; http://dx.doi.org/10.1016/j.febslet.2009.10.026
4. Pocard T, Le Bivic A, Galli T, Zurzolo C. Distinct v-SNAREs regulate direct and indirect apical delivery in polarized epithelial cells. J Cell Sci 2007; 120:3309-20; PMID:17878240; http://dx.doi.org/10.1242/jcs.007948
5. Martinez-Arca S, Coco S, Mainguy G, Schenk U, Alberts P, Bouille P, Mezzina M, Prochiantz A, Matteoli M, Louvard D, et al. A common exocytotic mechanism mediates axonal and dendritic outgrowth. J Neurosci 2001; 21:3830-8; PMID:11356871
6. Muzerelle A, Alberts P, Martinez-Arca S, Jeannequin O, Lafaye P, Mazie JC, Galli T, Gaspar P. Tetanus neurotoxin-insensitive vesicle-associated membrane protein localizes to a presynaptic membrane compartment in selected terminal subsets of the rat brain.

Neuroscience 2003; 122:59-75; PMID:14596849; http://dx.doi.org/10.1016/S0306-4522(03)00567-0

7. Advani RJ, Yang B, Prekeris R, Lee KC, Klumperman J, Scheller RH. VAMP-7 mediates vesicular transport from endosomes to lysosomes. J Cell Biol 1999; 146:765-76; PMID:10459012; http://dx.doi.org/10.1083/jcb.146.4.765

8. Luzio JP, Pryor PR, Gray SR, Gratian MJ, Piper RC, Bright NA. Membrane traffic to and from lysosomes. Biochem Soc Symp 2005:77-86; PMID:15649132

9. Pols MS, van Meel E, Oorschot V, ten Brink C, Fukuda M, Swetha MG, Mayor S, Klumperman J. hVps41 and VAMP7 function in direct TGN to late endosome transport of lysosomal membrane proteins. Nat Commun 2013; 4:1361; PMID:23322049; http://dx.doi.org/10.1038/ncomms2360

10. Proux-Gillardeaux V, Raposo G, Irinopoulou T, Galli T. Expression of the Longin domain of TI-VAMP impairs lysosomal secretion and epithelial cell migration. Biol Cell 2007; 99:261-71; PMID:17288539; http://dx.doi.org/10.1042/BC20060097

11. Verderio C, Cagnoli C, Bergami M, Francolini M, Schenk U, Colombo A, Riganti L, Frassoni C, Zuccaro E, Danglot L, et al. TI-VAMP/VAMP7 is the SNARE of secretory lysosomes contributing to ATP secretion from astrocytes. Biol Cell 2012; 104:213-28; PMID:22188132; http://dx.doi.org/10.1111/boc.201100070

12. Moreau K, Ravikumar B, Renna M, Puri C, Rubinsztein DC. Autophagosome precursor maturation requires homotypic fusion. Cell 2011; 146:303-17; PMID:21784250; http://dx.doi.org/10.1016/j.cell.2011.06.023

13. Fader CM, Sanchez DG, Mestre MB, Colombo MI. TI-VAMP/VAMP7 and VAMP3/cellubrevin: two v-SNARE proteins involved in specific steps of the autophagy/multivesicular body pathways. Biochim Biophys Acta 2009; 1793:1901-16; PMID:19781582; http://dx.doi.org/10.1016/j.bbamcr.2009.09.011

14. Galli T, Zahraoui A, Vaidyanathan VV, Raposo G, Tian JM, Karin M, Niemann H, Louvard D. A novel tetanus neurotoxin-insensitive vesicle-associated membrane protein in SNARE complexes of the apical plasma membrane of epithelial cells. Mol Biol Cell 1998; 9:1437-48; PMID:9614185; http://dx.doi.org/10.1091/mbc.9.6.1437

15. Lafont F, Verkade P, Galli T, Wimmer C, Louvard D, Simons K. Raft association of SNAP receptors acting in apical trafficking in Madin-Darby canine kidney cells. Proc Natl Acad Sci U S A 1999; 96:3734-8; PMID:10097106

16. Danglot L, Chaineau M, Dahan M, Gendron MC, Boggetto N, Perez F, Galli T. Role of TI-VAMP and CD82 in EGFR cell-surface dynamics and signaling. J Cell Sci 2010; 123:723-35; PMID:20144992; http://dx.doi.org/10.1242/jcs.062497

17. Charrin S, Manie S, Billard M, Ashman L, Gerlier D, Boucheix C, Rubinstein E. Multiple levels of interactions within the tetraspanin web. Biochem Biophys Res Commun 2003; 304:107-12; PMID:12705892; http://dx.doi.org/10.1016/S0006-291X(03)00545-X

18. Odintsova E, Butters TD, Monti E, Sprong H, van Meer G, Berditchevski F. Gangliosides play an important role in the organization of CD82-enriched microdomains. Biochem J 2006; 400:315-25; PMID:16859490; http://dx.doi.org/10.1042/BJ20060259

19. Hesketh GG, Perez-Dorado I, Jackson LP, Wartosch L, Schafer IB, Gray SR, McCoy AJ, Zeldin OB, Garman EF, Harbour ME, et al. VARP is recruited on to endosomes by direct interaction with retromer, where together they function in export to the cell surface. Dev Cell 2014; 29:591-606; PMID:24856514; http://dx.doi.org/10.1016/j.devcel.2014.04.010

20. Larghi P, Williamson DJ, Carpier JM, Dogniaux S, Chemin K, Bohineust A, Danglot L, Gaus K, Galli T, Hivroz C. VAMP7 controls T cell activation by regulating the recruitment and phosphorylation of vesicular Lat at TCR-activation sites. Nat Immunol 2013; 14:723-31; PMID:23666293; http://dx.doi.org/10.1038/ni.2609

21. De Matteis MA, Luini A. Exiting the Golgi complex. Nat Rev 2008; 9:273-84; PMID:18354421; http://dx.doi.org/10.1038/nrm2378

22. Korlach J, Schwille P, Webb WW, Feigenson GW. Characterization of lipid bilayer phases by confocal microscopy and fluorescence correlation spectroscopy. Proc Natl Acad Sci U S A 1999; 96:8461-6; PMID:10411897; http://dx.doi.org/10.1073/pnas.96.15.8461

23. Baumgart T, Hess ST, Webb WW. Imaging coexisting fluid domains in biomembrane models coupling curvature and line tension. Nature 2003; 425:821-4; PMID:14574408; http://dx.doi.org/10.1038/nature02013

24. Eggeling C, Ringemann C, Medda R, Schwarzmann G, Sandhoff K, Polyakova S, Belov VN, Hein B, von Middendorff C, Schönle A, et al. Direct observation of the nanoscale dynamics of membrane lipids in a living cell. Nature 2009; 457:1159-62; PMID:19098897; http://dx.doi.org/10.1038/nature07596

25. Marquer C, Leveque-Fort S, Potier MC. Determination of lipid raft partitioning of fluorescently-tagged probes in living cells by Fluorescence Correlation Spectroscopy (FCS). J Vis Exp 2012:e3513; PMID:22508446

26. D'Angelo G, Uemura T, Chuang CC, Polishchuk E, Santoro M, Ohvo-Rekila H, Sato T, Di Tullio G, Varriale A, D'Auria S, et al. Vesicular and non-vesicular transport feed distinct glycosylation pathways in the Golgi. Nature 2013; 501:116-20; PMID:23913272; http://dx.doi.org/10.1038/nature12423

27. Bankaitis VA, Garcia-Mata R, Mousley CJ. Golgi membrane dynamics and lipid metabolism. Curr Biol 2012; 22:R414-24; PMID:22625862; http://dx.doi.org/10.1016/j.cub.2012.03.004

28. Holthuis JC, Menon AK. Lipid landscapes and pipelines in membrane homeostasis. Nature 2014; 510:48-57; PMID:24899304; http://dx.doi.org/10.1038/nature13474

29. Boncompain G, Divoux S, Gareil N, de Forges H, Lescure A, Latreche L, Mercanti V, Jollivet F, Raposo G, Perez F. Synchronization of secretory protein traffic in populations of cells. Nat Methods 2012; 9:493-8; PMID:22406856; http://dx.doi.org/10.1038/nmeth.1928

30. Keller P, Toomre D, Diaz E, White J, Simons K. Multicolour imaging of post-Golgi sorting and trafficking in live cells. Nat Cell Biol 2001; 3:140-9; PMID:11175746; http://dx.doi.org/10.1038/35055042

31. Burgo A, Proux-Gillardeaux V, Sotirakis E, Bun P, Casano A, Verraes A, Liem RK, Formstecher E, Coppey-Moisan M, Galli T. A molecular network for the transport of the TI-VAMP/VAMP7 vesicles from cell center to periphery. Dev Cell 2012; 23:166-80; PMID:22705394; http://dx.doi.org/10.1016/j.devcel.2012.04.019

32. Presley JF, Cole NB, Schroer TA, Hirschberg K, Zaal KJ, Lippincott-Schwartz J. ER-to-Golgi transport visualized in living cells. Nature 1997; 389:81-5; PMID:9288971; http://dx.doi.org/10.1038/38891

33. Boncompain G, Perez F. Fluorescence-based analysis of trafficking in mammalian cells. Methods Cell Biol 2013; 118:179-94; PMID:24295307

34. Puig B, Altmeppen H, Glatzel M. The GPI-anchoring of PrP: Implications in sorting and pathogenesis. Prion 2014; 8:11-8; PMID:24509692

35. Griffiths G, Fuller SD, Back R, Hollinshead M, Pfeiffer S, Simons K. The dynamic nature of the Golgi complex. J Cell Biol 1989; 108:277-97; PMID:2537312; http://dx.doi.org/10.1083/jcb.108.2.277

36. Chia J, Goh G, Racine V, Ng S, Kumar P, Bard F. RNAi screening reveals a large signaling network controlling the Golgi apparatus in human cells. Mol Syst Biol 2012; 8:629; PMID:23212246; http://dx.doi.org/10.1038/msb.2012.59

37. Lin CC, Love HD, Gushue JN, Bergeron JJ, Ostermann J. ER/Golgi intermediates acquire Golgi enzymes by brefeldin A-sensitive retrograde transport in vitro. J Cell Biol 1999; 147:1457-72; PMID:10613904; http://dx.doi.org/10.1083/jcb.147.7.1457

38. Loizides-Mangold U, David FP, Nesatyy VJ, Kinoshita T, Riezman H. Glycosylphosphatidylinositol anchors regulate glycosphingolipid levels. J Lipid Res 2012; 53:1522-34; PMID:22628614

39. Burgo A, Sotirakis E, Simmler MC, Verraes A, Chamot C, Simpson JC, Lanzetti L, Proux-Gillardeaux V, Galli T. Role of Varp, a Rab21 exchange factor and TI-VAMP/VAMP7 partner, in neurite growth. EMBO Rep 2009; 10:1117-24; PMID:19745841; http://dx.doi.org/10.1038/embor.2009.186

40. Randhawa VK, Thong FS, Lim DY, Li D, Garg RR, Rudge R, Galli T, Rudich A, Klip A. Insulin and hypertonicity recruit GLUT4 to the plasma membrane of muscle cells by using N-ethylmaleimide-sensitive factor-dependent SNARE mechanisms but different v-SNAREs: role of TI-VAMP. Mol Biol Cell 2004; 15:5565-73; PMID:15469990; http://dx.doi.org/10.1091/mbc.E04-03-0266

41. Sakyo T, Kitagawa T. Differential localization of glucose transporter isoforms in non-polarized mammalian cells: distribution of GLUT1 but not GLUT3 to detergent-resistant membrane domains. Biochim Biophys Acta 2002; 1567:165-75; PMID:12488050; http://dx.doi.org/10.1016/S0005-2736(02)00613-2

42. Inoue M, Chiang SH, Chang L, Chen XW, Saltiel AR. Compartmentalization of the exocyst complex in lipid rafts controls Glut4 vesicle tethering. Mol Biol Cell 2006; 17:2303-11; PMID:16525015; http://dx.doi.org/10.1091/mbc.E06-01-0030

43. Ammar MR, Humeau Y, Hanauer A, Nieswandt B, Bader MF, Vitale N. The Coffin-Lowry Syndrome-Associated Protein RSK2 Regulates Neurite Outgrowth through Phosphorylation of Phospholipase D (PLD1) and Synthesis of Phosphatidic Acid. J Neurosci 2013; 33:19470-9; PMID:24336713; http://dx.doi.org/10.1523/JNEUROSCI.2283-13.2013

44. Kuribara H, Tago K, Yokozeki T, Sasaki T, Takai Y, Morii N, Narumiya S, Katada T, Kanaho Y. Synergistic activation of rat brain phospholipase D by ADP-ribosylation factor and rhoA p21, and its inhibition by Clostridium botulinum C3 exoenzyme. J Biol Chem 1995; 270:25667-71; PMID:7592744; http://dx.doi.org/10.1074/jbc.270.43.25667

45. Zhang GF, Patton WA, Lee FJ, Liyanage M, Han JS, Rhee SG, Moss J, Vaughan M. Different ARF domains are required for the activation of cholera toxin and phospholipase D. J Biol Chem 1995; 270:21-4; PMID:7814376; http://dx.doi.org/10.1074/jbc.270.1.21

46. Hemler ME. Tetraspanin proteins mediate cellular penetration, invasion, and fusion events and define a novel type of membrane microdomain. Annu Rev Cell Dev Biol 2003; 19:397-422; PMID:14570575

47. Kawakami Y, Kawakami K, Steelant WF, Ono M, Baek RC, Handa K, Withers DA, Hakomori S. Tetraspanin CD9 is a "proteolipid," and its interaction with alpha 3 integrin in microdomain is promoted by GM3 ganglioside, leading to inhibition of laminin-5-dependent cell motility. J Biol Chem 2002; 277:34349-58; PMID:12068006

48. Odintsova E, Voortman J, Gilbert E, Berditchevski F. Tetraspanin CD82 regulates compartmentalisation and ligand-induced dimerization of EGFR. J Cell Sci 2003; 116:4557-66; PMID:14576349; http://dx.doi.org/10.1242/jcs.00793

49. Sandvig K, Olsnes S. Effect of temperature on the uptake, excretion and degradation of abrin and ricin by HeLa cells. Exp Cell Res 1979; 121:15-25; PMID:446525; http://dx.doi.org/10.1016/0014-4827(79)90439-7

50. Matlin KS, Simons K. Reduced temperature prevents transfer of a membrane glycoprotein to the cell surface but does not prevent terminal glycosylation. Cell 1983; 34:233-43; PMID:6883510; http://dx.doi.org/10.1016/0092-8674(83)90154-X

51. Dunn WA, Hubbard AL, Aronson NN, Jr. Low temperature selectively inhibits fusion between pinocytic vesicles and lysosomes during heterophagy of 125I-asialofetuin by the perfused rat liver. J Biol Chem 1980; 255:5971–8; PMID:6155379

52. Sengupta D, Linstedt AD. Control of organelle size: the Golgi complex. Annu Rev Cell Dev Biol 2011; 27:57-77; PMID:21639798

53. Polishchuk R, Di Pentima A, Lippincott-Schwartz J. Delivery of raft-associated, GPI-anchored proteins to the apical surface of polarized MDCK cells by a transcytotic pathway. Nat Cell Biol 2004; 6:297-307; PMID:15048124; http://dx.doi.org/10.1038/ncb1109

54. D'Angelo G, Polishchuk E, Di Tullio G, Santoro M, Di Campli A, Godi A, West G, Bielawski J, Chuang CC, van der Spoel AC, et al. Glycosphingolipid synthesis requires FAPP2 transfer of glucosylceramide. Nature 2007; 449:62-7; PMID:17687330; http://dx.doi.org/10.1038/nature06097

55. Sato M, Yoshimura S, Hirai R, Goto A, Kunii M, Atik N, Sato T, Sato K, Harada R, Shimada J, et al. The role of VAMP7/TI-VAMP in cell polarity and lysosomal exocytosis in vivo. Traffic (Copenhagen, Denmark) 2011; 12:1383-93; PMID:21740490; http://dx.doi.org/10.1111/j.1600-0854.2011.01247.x

56. Danglot L, Zylbersztejn K, Petkovic M, Gauberti M, Meziane H, Combe R, Champy MF, Birling MC, Pavlovic G, Bizot JC, et al. Absence of TI-VAMP/Vamp7 leads to increased anxiety in mice. J Neurosci 2012; 32:1962-8; PMID:22323709; http://dx.doi.org/10.1523/JNEUROSCI.4436-11.2012

57. Yoshino A, Setty SR, Poynton C, Whiteman EL, Saint-Pol A, Burd CG, Johannes L, Holzbaur EL, Koval M, McCaffery JM, et al. tGolgin-1 (p230, golgin-245) modulates Shiga-toxin transport to the Golgi and Golgi motility towards the microtubule-organizing centre. J Cell Sci 2005; 118:2279-93; PMID:15870108; http://dx.doi.org/10.1242/jcs.02358

58. de Chaumont F, Dallongeville S, Chenouard N, Herve N, Pop S, Provoost T, Meas-Yedid V, Pankajakshan P, Lecomte T, Le Montagner Y, et al. Icy: an open bioimage informatics platform for extended reproducible research. Nat Methods 2012; 9:690-6; PMID:22743774; http://dx.doi.org/10.1038/nmeth.2075

59. Lam SM, Tong L, Duan X, Petznick A, Wenk MR, Shui G. Extensive characterization of human tear fluid collected using different techniques unravels the presence of novel lipid amphiphiles. J Lipid Res 2014; 55:289-98; PMID:24287120; http://dx.doi.org/10.1194/jlr.M044826